As mentioned in the previous section, the condensation of the rotational mode about the b axis induces phase V, which belongs to Γ_5 representation of phase I. The modulation patterns in a network at $z \simeq \frac{1}{4}$ are shown in Fig. 6, where the neighboring atoms are linked by lines. The opposite rotations of tetrahedra in two chains along the a axis can be interpreted as follows: $MnCl_4(x \simeq \frac{1}{4}, y \simeq 0.4)$ rotates clockwise about the b axis and counterclockwise about the c axis. Then the C(3)–Cl(3) distance becomes shorter than the C(4)—Cl(4) distance. If the shorter distance is preferable for C—H—Cl bonding, then $N(CH_3)_4(x \simeq \frac{1}{4}, y \simeq 0.1)$ rotates clockwise about the c axis. From Fig. 6, the C—H—Cl bond length is 3.76–3.84 Å. This bonding may be important for realizing the low-temperature structure.

The authors are grateful to Professor A. Okazaki and Dr Machida for the use of the four-circle diffractometer (Nonius CAD-4) and for invaluable help in the data collection at the Center of Advanced Instrumental Analysis, Kyushu University, Japan.

References

GESI, K. & OZAWA, K. (1984). *J. Phys. Soc. Jpn*, **53**, 627–634.
HAMILTON, W. C. (1965). *Acta Cryst.* **18**, 502–510.
HASEBE, K., MASHIYAMA, H., KOSHIJI, N. & TANISAKI, S. (1987). *J. Phys. Soc. Jpn*, **56**, 3543–3552.
HASEBE, K., MASHIYAMA, H. & TANISAKI, S. (1985). *Jpn J. Appl. Phys.* **24**, 802–804.
International Tables for X-ray Crystallography (1974). Vol. IV. Birmingham: Kynoch Press. (Present distributor Kluwer Academic Publishers, Dordrecht.)
MASHIYAMA, H. & TANISAKI, S. (1981). *J. Phys. Soc. Jpn*, **50**, 1413–1414.
MOROSIN, B. (1967). Quoted in Wiesner *et al.* (1967), p. 573.
SAKURAI, T. (1967). Editor. *Universal Crystallographic Computation Program System*. The Crystallographic Society of Japan, Tokyo, Japan.
SAWADA, S., SHIROISHI, Y., YAMAMOTO, A., TAKASHIGE, M. & MATSUO, M. (1978). *Phys. Lett. A*, **67**, 56–58.
SHIMIZU, H., ABE, N., KOKUBO, N., YASUDA, N. & FUJIMOTO, S. (1980). *Solid State Commun.* **34**, 363–368.
SHIMIZU, H., ABE, N., YASUDA, N., FUJIMOTO, S., SAWADA, S. & SHIROISHI, Y. (1979). *Jpn J. Appl. Phys.* **18**, 857.
TANISAKI, S. & MASHIYAMA, H. (1980). *J. Phys. Soc. Jpn*, **48**, 339–340.
WIESNER, J. R., SRIVASTAVA, R. C., KENNARD, C. H. L., DIVAIRA, M. & LINGAFELTER, E. C. (1967). *Acta Cryst.* **23**, 565–574.

Crystal Structures of Polynuclear Aromatic Hydrocarbons. Classification, Rationalization and Prediction from Molecular Structure

BY GAUTAM R. DESIRAJU

School of Chemistry, University of Hyderabad, PO Central University, Hyderabad 500 134, India

AND A. GAVEZZOTTI

Dipartimento di Chimica Fisica ed Elettrochimica e Centro CNR, Universita di Milano, via Golgi 19, 20133 Milano, Italy

Abstract

Polynuclear aromatic hydrocarbons crystallize in four basic structure types which may be clearly differentiated by energetic and geometrical criteria. The major motifs in these four prototypes are the stack, or layer, and the glide, or herringbone. A study of 32 representative hydrocarbons shows that the adoption of one or the other structure type depends on the relative importance of C···C and C···H interactions and therefore on the number and positioning of C and H atoms in the molecule. Consequently, it is possible to consider part of the molecular free surface as 'stack promoting' and the rest as 'glide promoting'. Individual C and H atoms in a molecule may be assigned stack and glide factors based only on their atomic connectivity. Using these factors, a predictive mapping from molecular to crystal structure is attempted. Based as they are on molecular shape, the packing criteria proposed here provide a simple classification scheme and, in some cases, may be used to predict the crystal structures of other planar aromatic hydrocarbons.

Introduction

A predictive understanding of the packing of molecular crystals has been considered increasingly important in areas as varied as solid-state chemistry, materials science and drug design. The concept of crystal engineering which describes the deliberate design of organic crystal structures for specific physical and chemical purposes has therefore elicited much interest (Schmidt, 1971; Thomas, 1974; Scheffer, 1987;

Desiraju, 1984, 1987a,b, 1989). Two approaches to crystal engineering have been recognized. In the first, a small number of crystal structures are examined in detail to determine empirical potential-energy functions that describe non-bonded interatomic interactions. This approach was pioneered by Kitaigorodskii (1973) and refined by methods such as those developed by Williams (Williams, 1974; Williams & Starr, 1977; Gavezzotti & Simonetta, 1982). The second approach, statistical in nature, generalizes from a large amount of crystallographic data and extrapolates from common geometrical motifs therein to derive new structures (Hagler & Leiserowitz, 1983; Sarma & Desiraju, 1986).

Both these approaches have their drawbacks. Rigorous calculations for organic crystals are still very difficult while the choice of the correct compounds for structural comparison is not always straightforward. We propose in this paper an approach based on the molecular structure of the compound, mainly its size and shape, since several recent studies have revealed that there must be simple relationships between these latter molecular properties and the crystal structure (Gavezzotti & Desiraju, 1988; Gavezzotti, 1989; Desiraju & Kishan, 1989). Although this approach builds mostly on previous experience (Williams, 1974; Williams & Starr, 1977; Hagler & Leiserowitz, 1983), it may in principle carry the seed of a simple theory to
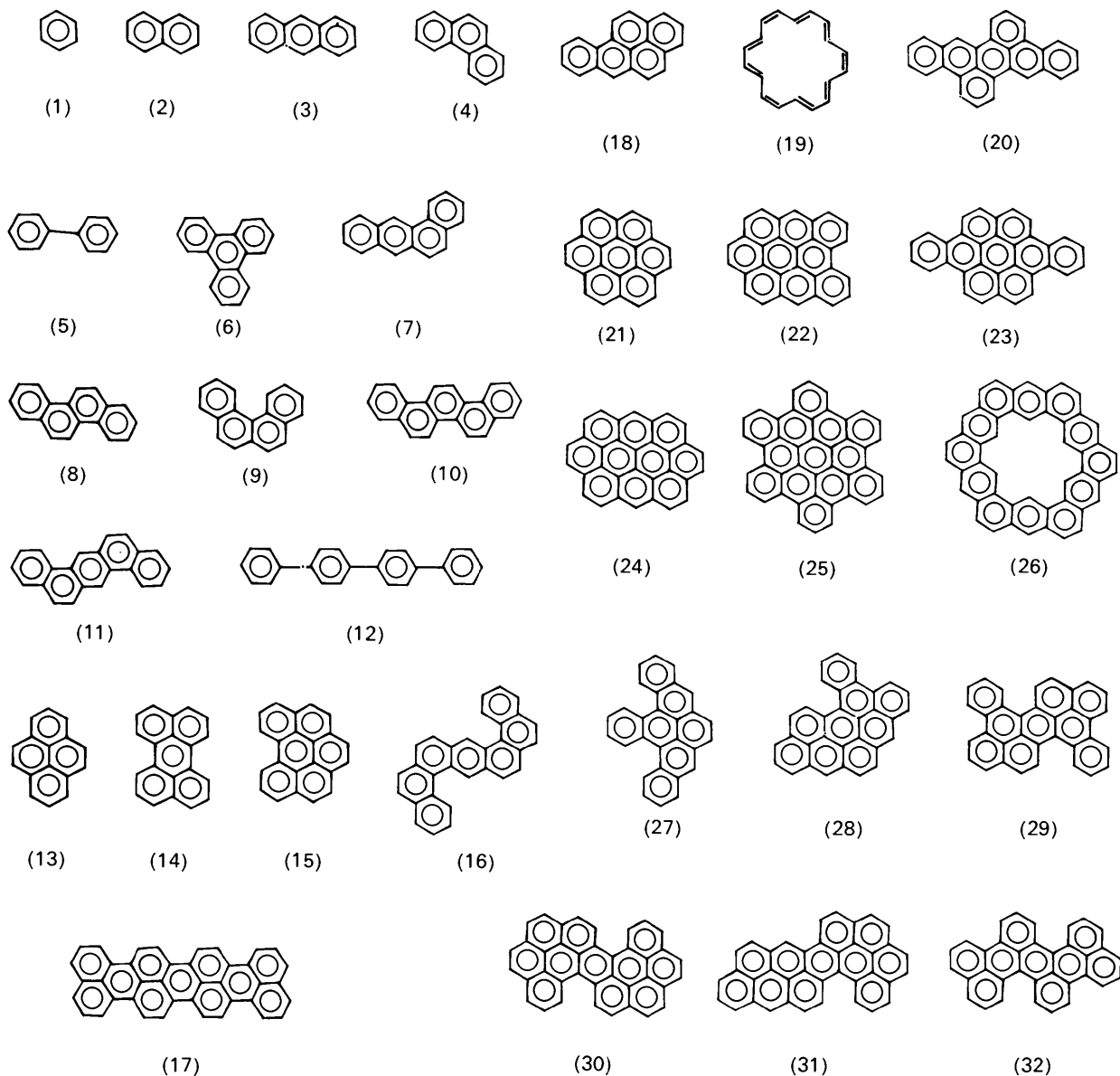

Fig. 1. Formulae of compounds (1)–(32).

obtain approximate crystal packings of a very large number of organic solids. Significantly, even such an approximate idea of an undetermined crystal structure often suffices for a clear understanding of many solid-state properties (Schmidt, 1964).

Structure types for aromatic hydrocarbons

The compounds we have analyzed in this paper, a series of polynuclear aromatic hydrocarbons [(1)–(32), Fig. 1] belong to one of the simplest yet most fundamental structural families. These compounds have been chosen since they adopt a few sharply defined packing types. They are planar or almost planar molecules and this lack of conformational flexibility allows a clear-cut definition of molecular shape.

The pioneering work of Robertson and his associates (Robertson, 1951) on the crystal structures of fused aromatic compounds was the starting point of our analysis. Robertson divided planar aromatic hydrocarbons into two categories. He recognized that when the molecules are disk-like with an area large compared to their thickness, they tend to stack in columns with a unit-cell axis of around 4·7 Å. Molecules of smaller area, which though still flat and disk-like, were observed to have a short cell axis greater than about 6 Å.

Kitaigorodskii also recognized various crystallization patterns for planar aromatic compounds (Kitaigorodskii, 1965, 1973). However, his analysis is more concerned with symmetry and close-packing aspects. While he was able to reproduce the observed orientation of molecules in hydrocarbon crystals through the device of pairwise atom potentials and generate new packings, given the unit-cell dimensions (Kitaigorodskii & Mirskaya, 1972), he did not really address the question of crystal structure prediction from molecular structure. The atom-potential method of Kitaigorodskii was further formalized (Williams, 1967, 1974; Williams & Starr, 1977; Mirsky, 1976). Using energetic as well as geometrical criteria and incorporating the observations of Kitaigorodskii and Williams, we now modify Robertson's classification to define four basic structural types for aromatic hydrocarbons. These four types may be clearly differentiated from one another. The simplest pattern that can be identified is the herringbone motif. In this structural type, C···C nonbonded interactions are between nonparallel nearest neighbour molecules. In the second type, called 'sandwich herringbone' or 'sandwich', the herringbone motif is made up of sandwich-type diads. In the third type, the main C···C interactions are between parallel translated molecules; a sort of flattened-out herringbone, called γ can be defined. All these structures also obtain crystal stabilization from C···H interactions. A fourth type is a layered structure made up of 'graphitic' planes. This is labelled β and is characterized by strong C···C interactions without much contribution from

C···H contacts. The terms β and γ are taken from the nomenclature of organic solid-state chemistry and follow from Schmidt's classification of trans-cinnamic acids (Schmidt, 1964). Fig. 2 shows packing diagrams of the four structure types. While the γ packing is seen to correspond to Robertson's first category, both sandwich and herringbone structures occur in his second group. We note further that β structures are not explicitly mentioned in his scheme.

Table 1 gives the 32 crystal structures in our database and Table 2 gives the literature citations for the structure determinations. This list of compounds, all of which contain only sp^2 carbon atoms, includes the simplest members of the family and also some unusual higher condensed aromatics. Some compounds have disordered or twinned structures but the main structure-defining features – cell parameters, crystal symmetries, molecular planes and their orientations – are available with enough accuracy for our purpose. None of our 32 compounds adopt triclinic packing; in fact the overwhelming majority are monoclinic. Significantly, the shortest crystallographic axis always coincides with the unique direction. For the five orthorhombic structures [(1), (6), (9), (27), (29)] the shortest axis corresponds to a screw direction. *The key parameters in separating the four structure types are therefore the shortest cell axis and the interplanar angle, defined as the angle between the mean plane of one molecule and that of its nearest neighbours.* These parameters define the molecular coordination. Fig. 2 shows convincingly that the shortest axis is in fact crystal structure defining while the two other cell axes are merely a function of individual molecular geometries.

Fig. 3 shows a plot of interplanar angle *versus* short axis. This plot sorts out the different populations; up to an axial value of 4 Å, one obtains β structures with very small interplanar angles. A relevant result of this analysis is that the region between short axis 4·2 and 4·6 Å is forbidden for planar aromatics. The γ structures cluster in the axial range 4·6–5·4 Å, while the domain of herringbone structures is between 5·4 and 8 Å with the monoclinic structures showing a clear
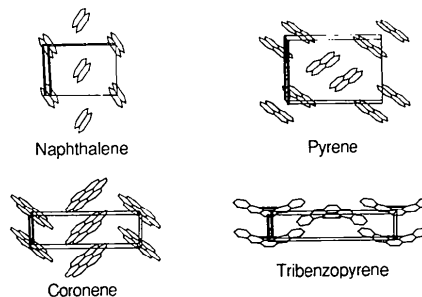

Fig. 2. The four basic aromatic crystal packings as exemplified by naphthalene (herringbone), coronene (γ), pyrene (sandwich) and tribenzopyrene (β).

Table 1. *Compounds considered in this study*

SA, shortest axis; S_g/S_{st} glide–stack ratio; S_M, molecular available surface area; IA, interplanar angle.

Compound	Formula	Space group	Z	SA (Å)	S_g/S_{st}	S_M (Å²)	IA (°)	(C/H)$_{surf}$
Herringbone structures								
(1) Benzene	C_6H_6	Pbca	4	6·92	2·21	108	88	1·65
(2) Naphthalene	$C_{10}H_8$	$P2_1/a$	2	5·97	2·09	154	52	1·83
(3) Anthracene	$C_{14}H_{10}$	$P2_1/a$	2	6·00	2·02	201	49	1·97
(4) Phenanthrene	$C_{14}H_{10}$	$P2_1$	2	6·16	1·99	198	58	2·00
(5) Biphenyl	$C_{12}H_{10}$	$P2_1/a$	2	5·58	2·05	184	64	1·92
(6) Triphenylene	$C_{18}H_{12}$	$P2_12_12_1$	4	5·26	1·88	239	80	2·23
(7) Benzanthracene	$C_{18}H_{12}$	$P2_1$	2	6·50	1·95	244	45	2·08
(8) Chrysene	$C_{18}H_{12}$	$I2/c$	4	5·78	1·92	241	58	2·14
(9) Benzo[c]phenanthrene	$C_{18}H_{12}$	$P2_12_12_1$	4	5·78	1·95	241	85	2·07
(10) Picene	$C_{22}H_{14}$	$P2_1$	2	6·15	1·87	285	58	2·24
(11) Dibenzanthracene	$C_{22}H_{14}$	$P2_1$	2	6·59	1·93	291	45	2·17
(12) Quaterphenyl	$C_{24}H_{18}$	$P2_1/a$	2	5·61	1·92	335	66	2·14
Sandwich herringbone structures								
(13) Pyrene	$C_{16}H_{10}$	$P2_1/a$	4	8·47	1·73	212	83	2·12
(14) Perylene	$C_{20}H_{12}$	$P2_1/a$	4	10·26	1·67	253	69	2·30
(15) Benzperylene	$C_{22}H_{12}$	$P2_1/a$	4	9·89	1·51	267	64	2·40
(16) Dinaphthoanthracene	$C_{30}H_{18}$	$P2_1/c$	4	8·16	1·88	375	62	2·24
(17) Quaterrylene	$C_{40}H_{20}$	$P2_1/a$	4	10·63	1·40	450	69	2·72
γ structures								
(18) Benzopyrene	$C_{20}H_{12}$	$P2_1/c$	4	4·53	1·71	255	73	2·21
(19) [18]Annulene	$C_{18}H_{18}$	$P2_1/a$	2	4·80	1·99	246	79	1·75
(20) Dibenzoperylene	$C_{28}H_{16}$	$A2/a$	4	5·23	1·65	341	81	2·44
(21) Coronene	$C_{24}H_{18}$	$P2_1/a$	2	4·70	1·40	281	85	2·44
(22) Benzobisanthrene	$C_{30}H_{14}$	Pa	4	4·68	1·30	337	—	2·63
(23) Dibenzocoronene	$C_{32}H_{16}$	$C2/c$	4	5·22	1·37	363	83	2·69
(24) Ovalene	$C_{32}H_{14}$	$P2_1/a$	2	4·70	1·24	351	86	2·70
(25) Hexabenzocoronene	$C_{42}H_{18}$	$P2_1/a$	2	5·11	1·09	439	86	3·19
(26) Kekulene	$C_{48}H_{24}$	$C2/c$	4	4·58	1·08	491	86	2·69
β structures								
(27) Tribenzopyrene	$C_{28}H_{16}$	$Pn2_1m$	2	4·02	1·69	340	30	2·31
(28) Violanthrene	$C_{34}H_{18}$	$P2_1/c$	4	3·80	1·42	395	—	2·54
(29) Tetrabenzoperylene	$C_{34}H_{18}$	$Pcab$	8	7·65	1·51	392	3	2·49
(30) Diphenanthroperylene	$C_{38}H_{18}$	$C2$	4	3·83	1·36	420	0	2·68
(31) Anthrabenzonaphthopentacene	$C_{38}H_{18}$	Pa	4	3·78	1·36	424	29	2·69
(32) Diperinaphthyleneanthracene	$C_{34}H_{18}$	$P2_1$	2	7·83	1·51	392	9	2·54

trend of decreasing interplanar angle with increasing short axis. Above a short axis value of 8 Å, the sandwich structures display a similar, if rather uncertain trend. Orthorhombic herringbone structures do not lend themselves to ready generalizations, benzene being an absolute outlier; in fact its molecular shape is not far from spherical and its crystal structure may be viewed as a distorted cubic packing of spheres.

Potential packing energies have been computed using atom–atom pairwise potentials as described previously (Gavezzotti & Desiraju, 1988) for all compounds for which a full structure determination is available. There has been a debate on whether the (6-exp) and similar formulations are adequate to quantitatively describe the intermolecular potential energy of aromatics, or whether the introduction of other terms in the potential expression is necessary (Kitaigorodskii, 1973, 1978; Williams, 1974; Williams & Starr, 1977). Our line of thought is in agreement with recent views (Pertsin & Kitaigorodskii, 1987) on nonbonded potentials in general; the use of optimized potentials which do not include explicit Coulomb terms does not mean that electrostatic interactions are altogether neglected. The potentials we use here have been shown to fit the static properties of aromatic crystals reasonably well and their adequacy is established from previous work

(Mirsky, 1976; Gavezzotti, 1982; Gavezzotti & Desiraju, 1988).

One of the advantages of our approach is that it is possible to sidestep such issues. These methodological problems only marginally concern us here, since we are attempting to recast crystal potentials and forces (whatever their origin and analytical expression) in the geometrical terms of shape and surface. In this context we need the potentials *only* to factor the total lattice energy into molecule-to-molecule contributions in the first coordination shell in the crystal. With such a treatment and using *any* reasonably well-parametrized intermolecular potential, it is easy to tell which crystals form molecular pairs since the interaction energy to one molecule (the sandwich partner) is unique. However, for crystals where the repeat unit is one molecule (herringbone, β, γ), there are always pairs of molecules with the same cohesion energy to the central reference molecule. Further, we have noted from such calculations that for β and γ structures, but not herringbone, stabilization is mainly by the two nearest short-axis-translated neighbours (Sarma & Desiraju, 1985; Gavezzotti & Desiraju, 1988). It is pertinent to record here that the total-energy considerations discriminate between structure types but poorly, since energy differences are always small and ill-determined. Energy

Table 2. *Numbering, name, REFCODE in the Cambridge files, and literature citation for the compounds in this study*

(1) Benzene (BENZEN) BACON, G. E., CURRY, N. A. & WILSON, S. A. (1964). *Proc. R. Soc. London Ser. A*, **279**, 98–110.
(2) Naphthalene (NAPHTA10) BROCK, C. P. & DUNITZ, J. D. (1982). *Acta Cryst.* **B38**, 2218–2228.
(3) Anthracene (ANTCEN) MASON, R. (1964). *Acta Cryst.* **17**, 547–555.
(4) Phenanthrene (PHENAN13) KAY, M. I., OKAYA, Y. & COX, D. E. (1971). *Acta Cryst.* **B27**, 26–33.
(5) Biphenyl (BIPHEN02) ROBERTSON, G. B. (1961). *Nature (London)*, **191**, 593–594.
(6) Triphenylene (TRIPHE11) FERRARIS, G., JONES, D. W. & YERKESS, J. (1973). *Z. Kristallogr.* **138**, 113–128.
(7) 1:2-Benzanthracene (BEANTR) FRIEDLANDER, P. H. & SAYRE, D. (1956). *Nature (London)*, **178**, 999–1000.
(8) Chrysene (CRYSEN) BURNS, D. M. & IBALL, J. (1960). *Proc. R. Soc. London Ser. A*, **257**, 491–514.
(9) Benzo[c]phenanthrene (BZPHAN) HIRSHFELD, F. L., SANDLER, S. & SCHMIDT, G. M. J. (1963). *J. Chem. Soc.* pp. 2108–2125.
(10) Picene (ZZZOYC01) DE, A., GHOSH, R., ROYCHOWDURY, S. & ROYCHOWDURY, P. (1985). *Acta Cryst.* **C41**, 907–909.
(11) Dibenz[a,h]anthracene (DBNTHR02) IBALL, J., MORGAN, C. H. & ZACHARIAS, D. E. (1975). *J. Chem. Soc. Perkin Trans.* pp. 1271–1272.
(12) p-Quaterphenyl (QUPHEN) DELUGEARD, Y., DESUCHE, J. & BAUDOUR, J. L. (1976). *Acta Cryst.* **B32**, 702–705.
(13) Pyrene (PYRENE02) HAZELL, A. C., LARSEN, F. K. & LEHMANN, M. S. (1972). *Acta Cryst.* **B28**, 2977–2984.
(14) Perylene (PERLEN01) CAMERMAN, A. & TROTTER, J. (1964). *Proc. R. Soc. London Ser. A*, **279**, 129–146.
(15) 1:12-Benzperylene (BNPERY) WHITE, J. G. (1948). *J. Chem. Soc.* pp. 1398–1408.
(16) Dinaphtho[1,2-a:1′,2′-h]anthracene (DNAPAN) HUMMELINK-PETERS, B. G. M. C., VAN DER HARK, T. E. M., NOORDIK, J. H. & BEURSKENS, P. T. (1975). *Cryst. Struct. Commun.* **4**, 281–284.
(17) Quaterrylene (QUATER10) KERR, K. A., ASHMORE, J. P. & SPEAKMAN, J. C. (1975). *Proc. R. Soc. London Ser. A*, **344**, 199–215.
(18) 3,4-Benzopyrene (BNPYRE10) IBALL, J., SCRIMGEOUR, S. N. & YOUNG, D. W. (1976). *Acta Cryst.* **B32**, 328–330.
(19) [18]Annulene (ANULEN) BREGMAN, J., HIRSHFELD, F. L., RABINOVICH, D. & SCHMIDT, G. M. J. (1965). *Acta Cryst.* **19**, 227–233.
(20) 2,3:8,9-Dibenzoperylene (DBPERY) LIPSCOMB, W. N., ROBERTSON, J. M. & ROSSMANN, M. G. (1959). *J. Chem. Soc.* pp. 2601–2607.
(21) Coronene (CORONE01) ROBERTSON, J. M. & WHITE, J. G. (1945). *J. Chem. Soc.* pp. 607–617.
(22) 1,14-Benzobisanthrene (BEANTH) TROTTER, J. (1958). *Acta Cryst.* **11**, 423–428.
(23) 1,2:7,8-Dibenzocoronene (DBZCOR) ROBERTSON, J. M. & TROTTER, J. (1961). *J. Chem. Soc.* pp. 1115–1120.
(24) Ovalene (OVALEN01) HAZELL, R. G. & PAWLEY, G. S. (1973). *Z. Kristallogr.* **137**, 159–172.
(25) 1,12:2,3:4,5:6,7:8,9:10,11-Hexabenzocoronene (HBZCOR) ROBERTSON, J. M. & TROTTER, J. (1961). *J. Chem. Soc.* pp. 1280–1284.
(26) Kekulene (KEKULN10) STAAB, A., DIEDERICH, F., KRIEGER, C. & SCHWEITZER, D. (1983). *Chem. Ber.* **116**, 3504.
(27) Tribenzopyrene (TBZPYR) ROBERTS, P. J. & FERGUSON, G. (1977). *Acta Cryst.* **B33**, 1244–1247.
(28) Violanthrene (CORXAI10) OONISHI, I., FUJISAWA, S. AOKI, J., OHASHI, Y. & SASADA, Y. (1986). *Bull. Chem. Soc. Jpn*, **59**, 2233.
(29) Tetrabenzo[a,cd,j,lm]perylene (TBZPER) KOHNO, Y., KOHNO, M., SAITO, Y. & INOKUCHI, H. (1975). *Acta Cryst.* **B31**, 2076–2080.
(30) Diphenanthro[5,4,3-abcd:5′,4′,3′-jklm]perylene (NAPPYR01) OONISHI, I., FUJISAWA, S., AOKI, J. & DANNO, T. (1978). *Bull. Chem. Soc. Jpn*, **51**, 2256–2260.
(31) Anthra[2,1,9,8-hijkl]benzo[de]naphtho[2,1,8,7-stuv]pentacene (BOXGAW) FUJISAWA, S., OONISHI, I., AOKI, J., OHASHI, Y. & SASADA, Y. (1982). *Bull. Chem. Soc. Jpn*, **55**, 3424.
(32) 1,9:5,10-Diperinaphthyleneanthracene (NAPANT) ROSSMAN, M. G. (1959). *J. Chem. Soc.* pp. 2607–2613.

calculations are used by us just as a quantification of the composition of the coordination sphere in the crystal and in this sense as a confirmation of our classification scheme.

From molecular to crystal structure: the free surface approach

We now analyze the molecular features which may lead to a particular crystal structure type for a given compound. The crucial link between molecular and crystal structure is the relative ability of a molecule to employ intermolecular C···C, C···H and H···H interactions. *These contacts have quite different orientational requirements* which have been consistently recognized in small-molecule and macromolecule crystal structures (Perutz, Fermi, Abraham, Poyart & Bursaux, 1986). These orientational requirements have been confirmed by *ab initio* calculations (Karlstrom, Linse, Wallqvist & Jonsson, 1983; Pawliszyn, Szczesniak & Scheiner, 1984) and molecular-beam studies of van der Waals complexes (Janda, Hemminger, Winn, Novick, Harris & Klemperer, 1975; Steed, Dixon & Klemperer, 1979). While C···C interactions are best optimized between parallel molecules stacked at van der Waals separation (π–π interactions), C···H interactions are most effective between inclined molecules. It has been argued that the inclined arrangement is stabilized since it brings the (+) hydrogen atom of an aromatic ring into close contact with the (−) electron cloud of the adjacent ring, in other words that the C···H interaction is better represented as C(δ−)···H(δ+) (Burley & Petsko, 1985). In the monoclinic milieu, such a geometry is most conveniently achieved by the use of glide planes and screw axes. So β and γ structures, where stacking is important, employ C···C interactions while herringbone structures, where glide stabilization is important, are characterized by C···H contacts (Sarma & Desiraju, 1985; Desiraju & Kishan, 1989). By this token, both C···C and C···H interactions are expected to be important for sandwich structures. Packing-energy calculations are of limited use in discussing this point since parameters are always optimized globally, rather than on separate contributions of atom types. Thus,
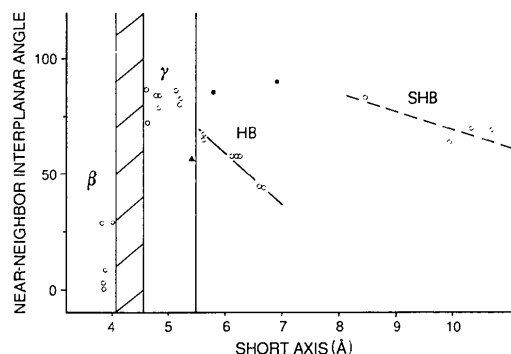

Fig. 3. Intermolecular interplanar angle (IA) (°) *versus* shortest cell axis (SA), in the crystal structures of the 32 condensed aromatics in Table 1. The black dots are the orthorhombic structures of benzene and triphenylene. The black triangle is the high-pressure monoclinic phase of benzene.

factoring of total energies into these contributions cannot be relied upon in an absolute sense: for naphthalene for example, %C⋯C is 58 or 65 and %H⋯H is 6 or 0·3 depending on whether the present functions or Williams (1967) functions are used, yet the sublimation energy is reproduced correctly by both parameter sets.

Clearly, an important molecular parameter affecting C⋯H versus C⋯C utilization, and therefore the choice of crystal structure, is the stoichiometric C/H ratio, $(C/H)_{st}$. Compounds (1)–(12) with smaller $(C/H)_{st}$ are more likely to use C⋯H interactions and to select herringbone packing. Conversely, compounds (18)–(32) tend to be either β or γ. Sandwich structures (13)–(17) are more enigmatic, being chosen by compounds with both low and high values of $(C/H)_{st}$. The exceptional herringbone structure of benzene with a very large short axis is a consequence of its very low $(C/H)_{st}$ value and of the great importance of C⋯H interactions. It is not surprising that naphthalene, with $(C/H)_{st} = 1·25$ is considered the archetype of the herringbone family, the 'NaCl of molecular crystals' (Kitaigorodskii, 1973).

We may also define a surface Ç/H ratio, $(C/H)_{surf}$, as:

$$(C/H)_{surf} = \Sigma(S_{a,i})_C / \Sigma(S_{a,i})_H$$

where the $S_{a,i}$ are the free atomic van der Waals surfaces, and have been calculated as described previously (Gavezzotti, 1983, 1985). This quantity $(C/H)_{surf}$, values of which are given in Table 1, is useful since there is a good correlation between molecular surface area and packing energy. Average values of $S_{a,i}$ which are, in effect, the incremental areas for carbon and hydrogen atoms of the type A, B_1, B_2, C, D and E are given in Table 3. These area increments are averaged over all available compounds to minimize errors in individual structure determinations. Inspection of this table and Fig. 4, however, shows that there is also a shape effect since the free surface of some of the outer atoms in a molecule may not be completely available for the establishment of intermolecular contacts if the atoms make close intramolecular approaches in strained molecular environments.

Since the relative number and positioning of C and H atoms in a molecule are the key features in defining the structure type, we extend our arguments and consider part of the molecular free surface as stack- (or layer-) promoting, and the rest of it as glide- (or herringbone-) promoting. Atoms that help stacking include core atoms (B_2) and part (50%) of the rim carbon atoms (A, B_1, C, D, E), while atoms that help glide packing include the other part (50%) of the rim carbon atoms and all hydrogen atoms. Atom labels and prescriptions for the free-surface apportioning are shown in Fig. 4. A, C, D and E carbon atoms bear hydrogens but not B_1 and B_2; while B_1 are peripheral, B_2 are inner carbon

Table 3. *Average atomic surface increments, $S_{a,i}$ (from the available molecular structures) and empirical availability factors*

Atom type	$S_{a,i}$	% Stack[a]	% Glide[b]	Availability factor[c]
C_1	10·8	50	50	1·00
C_{B_1}	5·8	50	50	1·00
C_{B_2}	5·8	100	0	1·00
C_C	11·2	50	50	1·00
C_D	10·4	50	50	0·67
C_E	9·2	50	50	0·50
H_A	6·8	0	100	1·00
H_C	6·8	0	100	1·00
H_D	5·6	0	100	0·67
H_E	5·1	0	100	0·50

Notes: (a) Total stack area per molecule $= 0·5$ ($10·8NA + 5·8NB_1 + 11·2NC + 0·67 \times 10·4ND + 0·50 \times 9·2NE$) $+ 5·8NB_2$, where NA, NB_1 etc. are the number of atoms of the type A, B_1 etc. Note that NA = number of C_A atoms = number of H_A atoms. (b) Total glide area per molecule $= 0·5(10·8NA + 5·8NB_1 + 11·2NC + 6·8NA + 6·8NC + 0·67 \times 5·6ND + 0·5 \times 5·1NE)$. (c) The availability factors are less then unity for intramolecularly sterically hindered atoms.

atoms and are entirely stack-promoting. The analysis finally requires that appropriate shielding factors be applied to D- and E-type atoms since they are partly unavailable for intermolecular contacts (Fig. 4). Summing the glide and stack contributions over all the atomic areas gives the overall glide- and stack-promoting areas S_g and S_{st}. All these breakdown and shielding factors are empirical but they have been obtained after a careful analysis of the crystal structures of compounds (1)–(32).

Fig. 5 shows the glide-to-stack ratio S_g/S_{st} as a function of the total molecular surface S_M ($S_M = S_g + S_{st}$). Several compounds |(33)–(43), Fig. 6| not included in the main set (1)–(32) have been considered: compounds (37)–(43) have not been characterized by
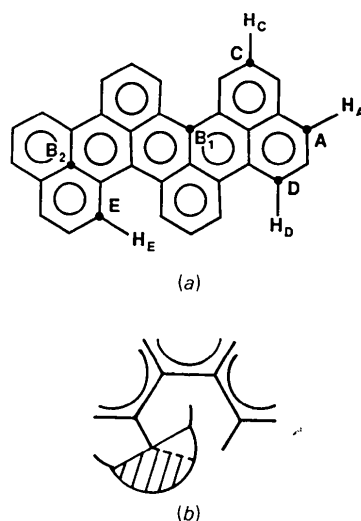

(a)

(b)

Fig. 4. (a) Labelling of C and H atoms for the assignment of area coefficients (Table 3). (b) Explanation of the partial availability of edge atoms. Only the shaded area is available for intermolecular contacts.

X-ray studies, and have been included as part of a predictive exercise. We will now discuss to what extent the plot constitutes a predictive mapping from molecular to crystal structure in that it can be supplied with a given structural formula to predict the crystal structure.

The plot gives a clear-cut division between herringbone structures and the rest. As expected, the former have the highest S_g/S_{st} values. The linear fused compounds [(1), (2), (3), (33), (34), (36)] and the linear polyphenyls [(1), (5), (35), (12)] form two smooth structural subgroups in this family. Other compounds deviate from these curves inasmuch as their shapes deviate from pseudolinearity. Thus, (4), (8) and (10) with a zigzag shape are further from the curves than the more linear (11). Compound (6) is almost an outlier in this line of thought.

The group of γ structures lies on a smooth curve in Fig. 5. The deviations of (18), (19), (21), (22), (24) and (26) from this curve are negligible, since all of them have roughly the same shape. Moving down this structurally homologous series there is an increase in 'core' carbon content, which means that the stack stabilization progressively increases. The similarity, approaching isomorphism, between (19) and (21) has already been alluded to (Bregman, Hirshfeld, Rabinovich & Schmidt, 1965); this similarity exists because inner H atoms are not involved in glide promotion. It is probably a moot question whether they are even relevant to crystal packing at all and our parameters for the evaluation of S_g/S_{st} can hardly be applied to (19) and (26). Compounds (20) and (23), which deviate the most from the disk-like shape, are also situated furthest from the curve. All these compounds are characterized by a highly condensed core of C atoms and a number of peripheral H atoms.
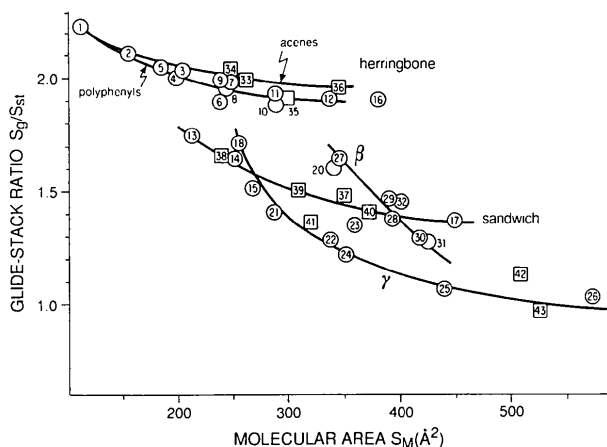
Since almost all these molecules are disc-shaped without internal contouring, they are also quite planar. This leads to good C$\cdots$C stacking but with an axial repeat of almost 4·7 Å, so that each molecular stack may dovetail with the adjacent one employing C$\cdots$H glide interactions (see Fig. 2). It seems therefore that the minimum short axis for effective C$\cdots$H interactions is around 4·7 Å.

The alternative arrangement for high C/H compounds is the β structure adopted by compounds (27)–(32). Here, C$\cdots$H interactions involving external H atoms are no longer possible. The notable geometrical difference between β and γ compounds is that all the β compounds are distorted from planarity making stack formation difficult. At the same time, the high C/H values imply that C$\cdots$C interactions must be important. A nonplanar molecule may still stack to optimize these, but to avoid excessive nonbonded repulsion, a large perpendicular stacking distance and a small degree of lateral offset (both relative to the γ structure; see Fig. 2) are necessary. Together, the above criteria imply short axes of around 4 Å. Since β molecules cannot be stacked at short axes much greater than 4 Å while γ molecules cannot be stacked at axial values less than 4·6 Å, the existence of a no-man's land between 4·0 and 4·6 Å may be understood.

The β structures (27)–(32) are bunched in a well-defined region in Fig. 5. Identification of a fused-ring hydrocarbon as a potential β structure is facile since, barring (9), only compounds which have
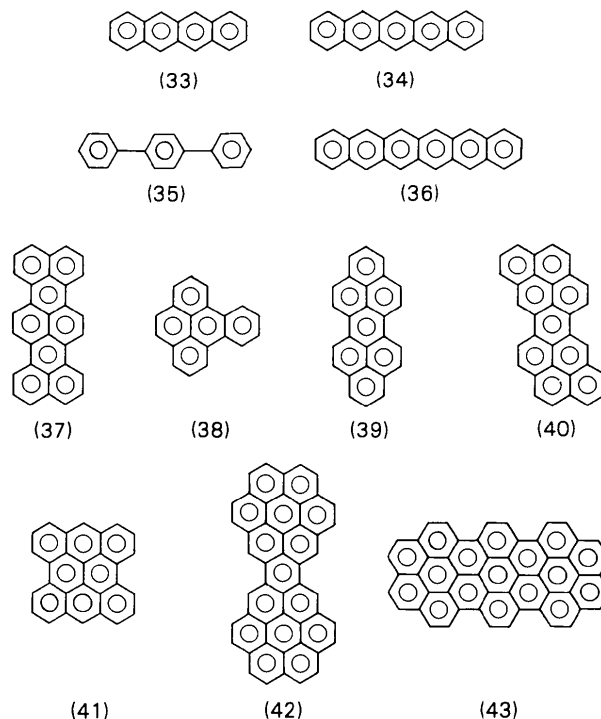

Fig. 5. A mapping from molecular to crystal structure for polynuclear aromatic hydrocarbons. Glide–stack area ratios are plotted against available molecular surface areas. Compounds (1)–(32) are shown as open circles and (33)–(43) as open squares.

Fig. 6. Formulae of compounds (33)–(43).

E-type carbons need be considered. The appearance of E-type atoms is accompanied by molecular nonplarity, which seems to be the key feature in discriminating between β and γ modes. We note further that β stacks are held loosely by H$\cdots$H interactions rather than by C$\cdots$H ones. Since these are weak, various crystallographic anomalies (disorder, two molecules in the asymmetric unit, supercells) are seen. H$\cdots$H interactions have not been taken into account in the calculation of glide and stack factors and H atoms have been assumed to lead always to C$\cdots$H interactions. Therefore, S_g/S_{st} values for (27)–(32) are probably not accurate.

Unlike the β structure which is quite distinct, the sandwich structure straddles the structural gap between herringbone and γ modes. As in γ packing, efficient C$\cdots$C stacking is found, but the stacked diads are held in a herringbone-like manner. Molecules (13), (14), (15) and (17) have both internal carbons and external hydrogens and their shapes are pallet- rather than disc-like. These geometrical features are manifested as S_g/S_{st} values intermediate between herringbone and γ compounds. Since both C$\cdots$C and C$\cdots$H interactions are important, both glide and stack stabilization are effective in this structure type.

Crystal structure prediction

We now proceed to use the predictive power of Fig. 5 for some compounds whose crystal structures are unknown, but are related to the ones discussed already. The crystal structure mapping plot of Fig. 5 shows that as S_M increases, all the curves slope downwards, since increasing molecular size usually means increasing the number of core atoms faster than the number of rim atoms; this is more so for disc-like molecules (β or γ crystal structures) whose curves have very negative slopes. These curves tend to converge at high carbon content; in contrast, cylinder-like molecules stay way up in S_g/S_{st} on increasing S_M, whether they have herringbone or sandwich structures. Therefore discrimination between γ and sandwich structures becomes easier at higher molecular weights. Separation between the curves is of course needed for a clear-cut crystal structure prediction; conversely, when several curves are close to each other, polymorphism becomes possible.

The sandwich compounds, perylene (14) and quaterrylene (17), both adopt the space group $P2_1/a$, with cell parameters of 11·35, 10·87, 10·37 and 11·14, 10·63, 19·23 Å, respectively, and β of 100·8 and 100·5°, respectively. The equality of the a axes reflects the similar molecular widths, while b is the structure-defining short axis. It may therefore be predicted that compound (37), which is intermediate between (14) and (17), will also adopt the space group $P2_1/a$ with cell parameters of 11·2, 10·5, 14·8 Å, $\beta = 100°$. Inciden-

tally, (37) is seen to lie exactly on the sandwich curve in Fig. 5. 1,2-Benzopyrene (38) may be derived from either (13) or (15), both of which have sandwich structures; its location in the plot is close to the sandwich curve, and almost matches (14). Therefore, it is predicted to adopt the sandwich mode. Dibenzoperylene (39) may be considered to belong to the series (14), (37), (17), all of which are sandwich structures and inspection of Fig. 5 shows it to lie exactly on the same curve. Dipyrene (40), is a dibenzo derivative of (39) and its structure may be either sandwich or γ, the former being more likely.

Dicoronylene (42), and the related hydrocarbons bisanthene (41) and hexabenzoquaterrylene (43), have a potential application in the formation of cation radical salts which might exhibit metallic conductivity (Lempka, Oberland & Schmidt, 1985). No crystallographic study is available, and an anticipation of the stacking patterns of these compounds is desirable. Compound (42) is, in fact, a tetrabenzoquaterrylene, but its shape is more disc-like than that of quaterrylene itself. S_g/S_{st} for (42) is therefore intermediate between sandwich and γ, perhaps slightly closer to the sandwich structure. The introduction of two more rings to give the even more disc-like (43) predictably shifts S_g/S_{st} still further towards the γ mode compound. (42) should therefore have the sandwich structure, while (43) may have a greater tendency to adopt the γ form. The lower hydrocarbon (41) is more elliptically shaped and closely related to ovalene (24). As such, its position lies exactly on the γ curve in Fig. 5 and its structure should correspond to this form.

Fig. 5 still has some fuzzy features, but summarizes in an efficient way the crystal packing and basic structural profile of large flat molecules. However, a number of obscure points still remain. For example, compound (11) also exists in an orthorhombic form which is quite different from the monoclinic one and the short-axis–interplanar-angle relationships described in Fig. 3 do not hold for this modification. Indeed, this appears to be a general problem for any orthorhombic structure. Perylene (14) has a herringbone polymorph besides the sandwich structure considered here (Tanaka, 1963). It may be argued that polymorphism in the normal temperature and pressure range is perhaps possible only in a limited range of molecular surface (say, from about 230 to 250 Å^2), since this is the range in Fig. 5 which shows a crossing and intersection of the various structural curves. In spite of all this, one can safely state that our structure-predicting graph will indicate the most probable if not all the possible crystal structures for a given fused aromatic hydrocarbon and in this respect we believe that its predictive power is still a very valuable one. Going further, one could state that Fig. 5 should predict the most thermodynamically stable structure for a given polynuclear aromatic hydrocarbon.

Summary and perspectives

We have analyzed and classified 32 representative crystal structures for condensed aromatic compounds and recognize four basic crystal structure types, herringbone, sandwich herringbone, β and γ. These types may be distinguished by structural parameters such as the shortest cell axis and interplanar angles. The shortest axis in particular is characteristic of the crystal packing since it always corresponds to the monoclinic or screw-axis direction. Molecular areas have been computed as the sum of atomic areas. Each atom in these molecules has been assigned a distinct 'stacking ability' and a 'glide-forming ability' on the basis of its position and connectivity in the molecule. A plot of the ratio of the total stacking and glide-forming surfaces *versus* the total molecular surface is given; it is, to our knowledge, the first attempt at a real mapping of crystal structure in terms of molecular structure for non-hydrogen-bonded crystals. Using this plot, a number of such predictions have been made for compounds whose crystal structures are unavailable.

There is another aspect of our analysis that may extend its validity. Since the structural features of each molecule have been consolidated in a sort of overall shape descriptor, it may be expected that whenever this shape is found in organic compounds, the effects on crystal structure should be the same, even if the compound is not a pure aromatic hydrocarbon. For example, any elongated molecule with H atoms on the rim and a surface area not higher than 250 Å^2 is expected to pack in a herringbone pattern; this indeed is the case for several dimethylnaphthalenes (Destro & Gavezzotti, 1989) and also for dibenzofuran (Reppart, Gallucci, Lundstedt & Gerkin, 1984), carbazole (Gerkin & Reppart, 1986) and fluorene (Gerkin, Lundstedt & Reppart, 1984). On the other hand, compound (44) (Fig. 7) misses H atoms in the rim, and therefore adopts a sandwich crystal structure (Destro, Pilati & Simonetta, 1977). While compound (45) has a typical γ- or β-producing shape, its crystal structure

(Toriumi, Koyano, Sato, Takaya, Ito & Inokuchi, 1982) is β-like since peripheral H atoms have been removed in the process of replacing C atoms by N. Again, while (46) has herringbone packing, (47) and (48) have a β structure for the same reason (Sarma & Desiraju, 1987). Similarly, the tendency for a substituted phenylpropiolic acid Ar—C≡C—CO$_2$H to adopt a β structure is always greater than the corresponding cinnamic acid, Ar—CH=CH—CO$_2$H (Desiraju & Kishnan, 1989). These examples show how the ideas we have described here may be adapted and extended to apply to a much wider range of molecular compounds. Since our approach is very general and conceptually simple, it is expected that it will be valid for more-polar derivatives. Accordingly, a search for other crystal-structure-defining parameters for organic compounds will be the subject of future work.

References

BREGMAN, J., HIRSHFELD, F. L., RABINOVICH, D. & SCHMIDT, G. M. J. (1965). *Acta Cryst.* 19, 227–234.
BURLEY, S. K. & PETSKO, G. (1985). *Science*, 229, 23–28.
DESIRAJU, G. R. (1984). *Endeavour*, 8, 201–206.
DESIRAJU, G. R. (1987a). Editor. *Organic Solid State Chemistry*. Amsterdam: Elsevier.
DESIRAJU, G. R. (1987b). *Prog. Solid State Chem.* 17, 295–353.
DESIRAJU, G. R. (1989). *Crystal Engineering. The Design of Organic Solids.* Amsterdam: Elsevier.
DESIRAJU, G. R. & GAVEZZOTTI, A. (1989). *J. Chem. Soc. Chem. Commun.* pp. 621–623.
DESIRAJU, G. R. & KISHAN, K. V. R. (1989). *J. Am. Chem. Soc.* 111. In the press.
DESTRO, R. & GAVEZZOTTI, A. (1989). Unpublished results.
DESTRO, R., PILATI, T. & SIMONETTA, M. (1977). *Acta Cryst.* B33, 447–456.
GAVEZZOTTI, A. (1982). *Nouv. J. Chim.* 6, 443–450.
GAVEZZOTTI, A. (1983). *J. Am. Chem. Soc.* 105, 5220–5225.
GAVEZZOTTI, A. (1985). *J. Am. Chem. Soc.* 107, 962–967.
GAVEZZOTTI, A. (1989). *J. Am. Chem. Soc.* 111, 1835–1843.
GAVEZZOTTI, A. & DESIRAJU, G. R. (1988). *Acta Cryst.* B44, 427–434.
GAVEZZOTTI, A. & SIMONETTA, M. (1982). *Chem. Rev.* 82, 1–13.
GERKIN, R. E., LUNDSTEDT, A. P. & REPPART, W. J. (1984). *Acta Cryst.* C40, 1892–1894.
GERKIN, R. E. & REPPART, W. J. (1986). *Acta Cryst.* C42, 480–482.
HAGLER, A. & LEISEROWITZ, L. (1983). *Proc. R. Soc. London Ser. A*, 388, 133–175.
JANDA, K. C., HEMMINGER, J. C., WINN, J. S., NOVICK, S. E., HARRIS, S. J. & KLEMPERER, W. (1975). *J. Chem. Phys.* 63, 1419–1421.
KARLSTROM, G., LINSE, P., WALLQVIST, A. & JONSSON, B. (1983). *J. Am. Chem. Soc.* 105, 3777–3782.
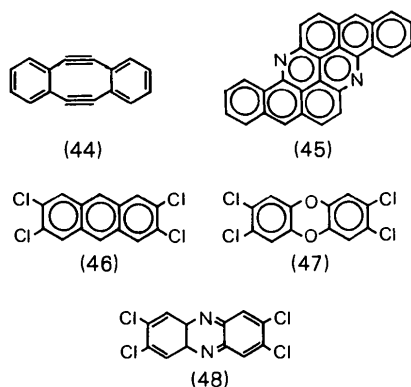KITAIGORODSKII, A. I. (1965). *Acta Cryst.* 18, 585–590.

(44)

(45)

(46)

(47)

(48)

Fig. 7. Formulae of compounds (44)–(48).

KITAIGORODSKII, A. I. (1973). *Molecular Crystals and Molecules.* New York: Academic Press.

KITAIGORODSKII, A. I. (1978). *Chem. Soc. Rev.* 7, 133–163.

KITAIGORODSKII, A. I. & MIRSKAYA, K. V. (1972). *Mater. Res. Bull.* 7, 1271–1280.

LEMPKA, H. J., OBERLAND, S. & SCHMIDT, W. (1985). *Chem. Phys.* 96, 349–360.

MIRSKY, K. (1976). *Acta Cryst.* A32, 199–207.

PAWLISZYN, J., SZCZESNIAK, M. M. & SCHEINER, S. (1984). *J. Phys. Chem.* 88, 1726–1730.

PERTSIN, A. J. & KITAIGORODSKII, A. I. (1987). *The Atom–Atom Potential Method,* pp. 74–75. Berlin: Springer-Verlag.

PERUTZ, M. F., FERMI, G., ABRAHAM, D. J., POYART, C. & BURSAUX, E. (1986). *J. Am. Chem. Soc.* 108, 1064–1078.

REPPART, W. J., GALLUCCI, J. C., LUNDSTEDT, A. P. & GERKIN, R. E. (1984). *Acta Cryst.* C40, 1572–1576.

ROBERTSON, J. M. (1951). *Proc. R. Soc. London Ser. A,* 207, 101–110.

SARMA, J. A. R. P. & DESIRAJU, G. R. (1985). *Chem. Phys. Lett.* 117, 160–164.

SARMA, J. A. R. P. & DESIRAJU, G. R. (1986). *Acc. Chem. Res.* 19, 222–228.

SARMA, J. A. R. P. & DESIRAJU, G. R. (1987). *J. Chem. Soc. Perkin Trans.* 2, pp. 1195–1202.

SCHEFFER, J. R. (1987). Editor. *Organic Chemistry in Anisotropic Media,* Tetrahedron Symposium-in-Print, No. 29. Oxford: Pergamon.

SCHMIDT, G. M. J. (1964). *J. Chem. Soc.* pp. 2014–2021.

SCHMIDT, G. M. J. (1971). *Pure Appl. Chem.* 27, 647–678.

STEED, J. M., DIXON, T. A. & KLEMPERER, W. (1979). *J. Chem. Phys.* 70, 4940–4946.

TANAKA, J. (1963). *Bull. Chem. Soc. Jpn,* 36, 1237–1249.

THOMAS, J. M. (1974). *Philos. Trans. R. Soc. London Ser. A,* 277, 251–286.

TORIUMI, K., KOYANO, K., SATO, N., TAKAYA, H., ITO, T. & INOKUCHI, H. (1982). *Acta Cryst.* B38, 959–961.

WILLIAMS, D. E. (1967). *J. Chem. Phys.* 45, 3770–3778.

WILLIAMS, D. E. (1974). *Acta Cryst.* A30, 71–77.

WILLIAMS, D. E. & STARR, T. L. (1977). *Comput. Chem.* 1, 173–177.

A Comparison of Laue and Monochromatic X-ray Analyses of a Small-Molecule Crystal

BY D. GOMEZ DE ANDEREZ*

Department of Physics, University of York, Heslington, York YO1 5DD, England

M. HELLIWELL*

Department of Chemistry, University of York, Heslington, York YO1 5DD, England

J. HABASH*

Department of Physics, University of York, Heslington, York YO1 5DD, England

E. J. DODSON

Department of Chemistry, University of York, Heslington, York YO1 5DD, England

J. R. HELLIWELL*†

Department of Physics, University of York, Heslington, York YO1 5DD, England, and SERC, Daresbury Laboratory, Daresbury, Warrington, Cheshire WA4 4AD, England

AND P. D. BAILEY AND R. E. GAMMON

Department of Chemistry, University of York, Heslington, York YO1 5DD, England

Abstract

As part of the development of the Laue method for quantitative structure analysis we report on a detailed comparison of monochromatic (Mo $K\alpha$ and Cu $K\alpha$) and synchrotron radiation Laue data from the same crystal of a small molecule, (*S*)-2-chloro-2-fluoro-*N*-[(*S*)-1-phenylethyl]ethanamide, $C_{10}H_{11}ClFNO$. The small-molecule crystal was non-centrosymmetric, space group $P2_12_12_1$ ($a = 5\cdot418$, $b = 12\cdot030$, $c = 15\cdot837$ Å), and contained a single Cl atom which is a weak anomalous scatterer as well as 13 other non-H atoms (C, N, O, F). The data sets

* Present address: Department of Chemistry, University of Manchester, Manchester M13 9PL, England.

† Author to whom correspondence should be addressed.